Resonances in 11C observed in the 4He(7Be, α)7Be and 4He(7Be, p)10B reactions

Freer, M.; Achouri, N. L.; Angulo, C.; Ashwood, N. I.; Bardayan, D. W.; Brown, S.; Catford, W. N.; Chipps, K. A.; Curtis, N.; Demaret, P.; ...

Repository / Repozitorij:

Repository of the Faculty of Science - University of Zagreb

Resonances in ^{11}C observed in the ^{4}He(^{7}Be, α)^{7}Be and ^{4}He(^{7}Be, p)^{10}B reactions

M. Freer,[1] N. L. Achouri,[2] C. Angulo,[3,*] N. I. Ashwood,[1] D. W. Bardayan,[4] S. Brown,[5] W. N. Catford,[5] K. A. Chipps,[6] N. Curtis,[1] P. Demaret,[3] C. Harlin,[5] B. Laurent,[2] J. D. Malcolm,[1] M. Milin,[7] T. Munoz-Britton,[1] N. A. Orr,[2] S. D. Pain,[4] D. Price,[1] R. Raabe,[8] N. Soić,[9] J. S. Thomas,[5] C. Wheldon,[1] G. Wilson,[5] and V. A. Ziman[1]

[1]*School of Physics and Astronomy, University of Birmingham, Edgbaston, Birmingham B15 2TT, UK*
[2]*Laboratoire de Physique Corpusculaire, ISMRA and Université de Caen, IN2P3-CNRS, F-14050 Caen Cedex, France*
[3]*CRC/LLN Centre de Recherches du Cyclotron, Université Catholique de Louvain, B-1348 Louvain-la-Neuve, Belgium*
[4]*Physics Division, Oak Ridge National Laboratory, MS-6354, Bldg. 6010, P.O. Box 2008, Oak Ridge, Tennessee 37831-6354, USA*
[5]*School of Electronics and Physical Sciences, University of Surrey, Guildford, Surrey GU2 7XH, UK*
[6]*Department of Physics and Astronomy, Rutgers, The State University of New Jersey, 136 Frelinghuysen Road, Piscataway, New Jersey 08854-8019 USA*
[7]*Department of Physics, Faculty of Science, University of Zagreb, Bijenicka 32, HR-10000 Zagreb, Croatia*
[8]*Instituut voor Kern- en Stralingsfysica, Katholieke Universiteit Leuven, B-3001 Leuven, Belgium*
[9]*Rudjer Bošković Institute, Department of Experimental Physics, Bijenička 54, HR-10000 Zagreb, Croatia*

Measurements of the ^{4}He(^{7}Be, α)^{7}Be and ^{4}He(^{7}Be, p)^{10}B reactions were performed using ^{7}Be beam energies of 7.1 and 23 MeV and a helium-4 target, employing the thick target technique. Resonances were observed between $E_x(^{11}$C$) = 8.6$ to 13.8 MeV. An R-matrix analysis was performed to characterize the spins and partial widths. This analysis showed that the observed sequence of states was consistent with that found for ^{7}Li $+ \alpha$ resonant scattering populating resonances in ^{11}B. A comparison of the proposed partial widths for decay with the Wigner limit indicates that several of the states are associated with cluster-like structures.

PACS number(s): 21.10.−k, 25.55.Hp, 25.70.Hi, 27.20.+n

I. INTRODUCTION

Correlations have a preeminent role in the determination of the structure of both heavy and light nuclei. In light nuclear systems, correlations, for example, those associated with the pairing interaction, dominate to the extent that the nucleus clusterizes. For example, the ^{8}Be nucleus is well known to have an α-α cluster structure as measured through its large reduced α-decay width and rotational behavior. Sophisticated *ab initio* calculations using the Green's function Monte Carlo approach, which are sensitive to such nucleon-nucleon correlations, reveal the two-α cluster structure [1].

The addition of a further α particle presents the opportunity for the formation of three-center cluster structures in ^{12}C. For example, the 3α cluster structure of the Hoyle state at 7.65 MeV has been well documented (e.g., Ref. [2]). The removal of a neutron or a proton yields ^{11}C and ^{11}B, respectively. The analogs of the 3α cluster states in these nuclei have been explored in Ref. [3]. Similarly, cluster structures are found within the framework of a cluster model [4] and antisymmetrized molecular dynamics [5] (which considers the interaction of all 11 nucleons with an effective interaction).

From an experimental perspective the ^{16}O(^{9}Be,^{7}Be $+ \alpha$)^{14}C and ^{7}Li(^{9}Be,^{7}Li $+ \alpha$)^{5}He reactions have been used to characterize α-decaying states in ^{11}C and ^{11}B [6] and α-decay widths of ^{11}B excited states were reported in Ref. [7]. Most recently, a measurement of the ^{7}Li $+ \alpha$ resonant scattering has

characterized the excitation energy spectrum of ^{11}B up to an excitation energy of 13 MeV [8].

Here we present measurements of the resonant scattering ^{7}Be $+ \alpha$ reaction, which is the analog to ^{7}Li $+ \alpha$. Information regarding the energies, spins, and widths of the unbound states above the α-decay threshold are obtained. These data permit a detailed comparison between ^{11}C and ^{11}B states populated in the two reactions and the determination of states with a cluster character.

II. EXPERIMENTAL DETAILS

The technique of resonance scattering using a thick target was first developed at the Kurchatov Institute [9]. It involves the passage of a beam through a target material. As the beam slows down and the center-of-mass energy coincides with that of a resonance of the composite system then a resonant component to the scattering process occurs. Typically, the target is a lighter mass than the projectile and the beam then stops in the target, so the resonant decay by light particle emission may be observed at zero degrees. This technique is appropriate for the characterization of proton and α-decay widths of excited states. In the present case, a thick helium-4 target was used with a ^{7}Be beam with silicon detectors in the forward direction to pick up the proton and α decay of ^{11}C resonances. For such an arrangement, resonances are formed at different depths in the gas volume, and hence the solid angle varies with excitation energy. Furthermore, the decay of a resonance to excited states in the products can contribute to the energy spectrum of the detected particles. These latter two features complicate the analysis.

*Current address: Tractebel Engineering, Avenue Ariane 7, B-1200 Brussels, Belgium.
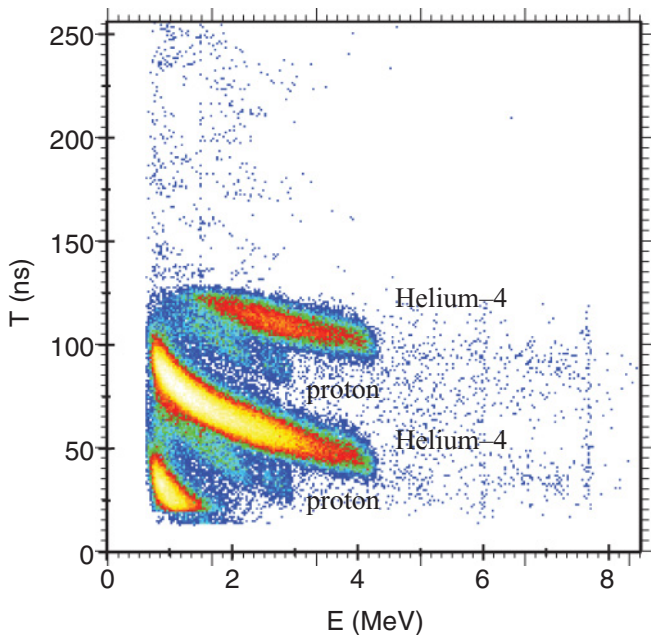
FIG. 1. (Color online) Energy vs time-of-flight spectrum, for all strips of the LEDA array, showing the identification of α particles and protons. The various particle types are labeled.

The measurements presented here are the combination of two experimental studies. The first of these was performed at Louvain-la-Neuve (LLN) and the second at Oak Ridge National Laboratory (ORNL).

For the LLN measurement, the ^{7}Be beam was produced using the two-accelerator technique. The ^{7}Be was produced by first irradiating a natural lithium target with a beam of 27-MeV protons and then the ^{7}Be ($T_{1/2} = 53.2$ days) was chemically separated and installed into an ion source. The ^{7}Be nuclei were accelerated to 7.1 MeV with an intensity of 5×10^7 pps.

The beam then passed through a 2.5-μm-thick Mylar window, losing 1.1 MeV. The window isolated a helium-4 gas volume from the beamline. The path length of the beam through the gas was 69 cm and measurements of the energy loss of the beam at pressures of 21, 40, 60, 80, 90, and 95 mbar were used to characterize the energy-loss characteristics. For the resonant scattering measurements the helium gas was maintained at a pressure of 110 mbar. The silicon array used for the measurements was housed within the gas volume. The array was arranged in a LEDA-type configuration [10] composed of 8 YY1-type silicon strip detectors [11] of thickness 500 μm. The plane of the array was placed 69 cm from the entrance window and the detectors covered a range of angles from 4.1° to 10.7° with respect to the chamber window, divided into 16 annular strips. The detectors were calibrated using α-source measurements. The energy resolution averaged over the entire array was ~100 keV.

The time of flight with respect to the cyclotron radio-frequency (rf) signal was also measured. This permitted different particle types to be distinguished. Figure 1 shows an energy versus time-of-flight (ToF) plot, which gives multiple loci corresponding to α particles and protons. Each particle type is represented by several loci due to the ToF electronic

window exceeding the cyclotron rf period. For the analysis presented here the complete α-particle and proton loci between times of 25 and 110 ns were used, with software gates placed around the two loci.

The second set of measurements was also performed using a previously prepared ^{7}Be sample placed in the ion source of the HRIBF tandem accelerator at ORNL. The 23-MeV ^{7}Be beam had an intensity of 5×10^4 pps and passed through a 5-μm-thick Havar window (losing 4.2 MeV) before passing through 38 cm of helium-4 gas at a pressure of 920 mbar. The ^{7}Be beam was eventually stopped in a Mylar foil of thickness 15 μm. Directly behind the foil were two 1-cm-diameter silicon detectors of thickness 100 and 200 μm. These formed a ΔE-E particle identification telescope. The telescope was capable of distinguishing protons from heavier elements, e.g., α particles. The detectors were energy calibrated using ^{241}Am and ^{244}Cm α sources. The energy calibration was confirmed at higher energies using the energies at which protons, deuterons, tritons, and α particles, produced in reactions with the beryllium beam, punch through the silicon detectors (i.e., cease to deposit their full energy).

III. ANALYSIS AND RESULTS

A. $E_{\text{beam}} = 7.1$ MeV

The proton and α-particle spectra using the 7.1-MeV beam, taken from the LEDA detectors, are shown in Fig. 2. Note that here these particles are not measured precisely at 0°, unlike the data taken at 23 MeV. The spectra correspond to the energies as measured in the silicon detectors (i.e., before correcting for the energy loss through the gas). The vertical dashed lines, in both parts of the figure, correspond to the maximum-energy protons and α particles which may be detected from the ^{7}Be + α interaction. In the case of the α particles the maximum energy observed is very close to the calculated value [Fig. 2(b)], whereas the proton spectrum [Fig. 2(a)] shows protons with energies in excess of that which are possible via the ^{4}He(^{77}Be, p)^{10}B reaction ($Q = -1.145$ MeV). These higher energy protons originate from the ^{1}H(^{7}Be, p) reaction on hydrogen in the Mylar entrance window. The vertical solid lines indicate the calculated range of proton energies from this source, confirming their origin. These higher energy protons have been eliminated from the analysis presented below.

The variation in the detector acceptance (including both kinematics and solid angle) with the distance of the interaction from the chamber window was calculated using a Monte Carlo simulation of the reaction and detection processes, including the energy loss through the gas. The proton and α-particle spectra were then normalized by dividing with the calculated acceptance. For the purpose of these calculations the emission angle of either the proton or the α particle in the ^{11}C center-of-mass frame was assumed to be isotropic. The corresponding ^{11}C excitation energies were then calculated from the proton and α-particle energies based on the energy loss of these particles and the beam through the gas; those were obtained using the energy loss code DEDX [12]. The reaction cross sections were then calculated by normalizing
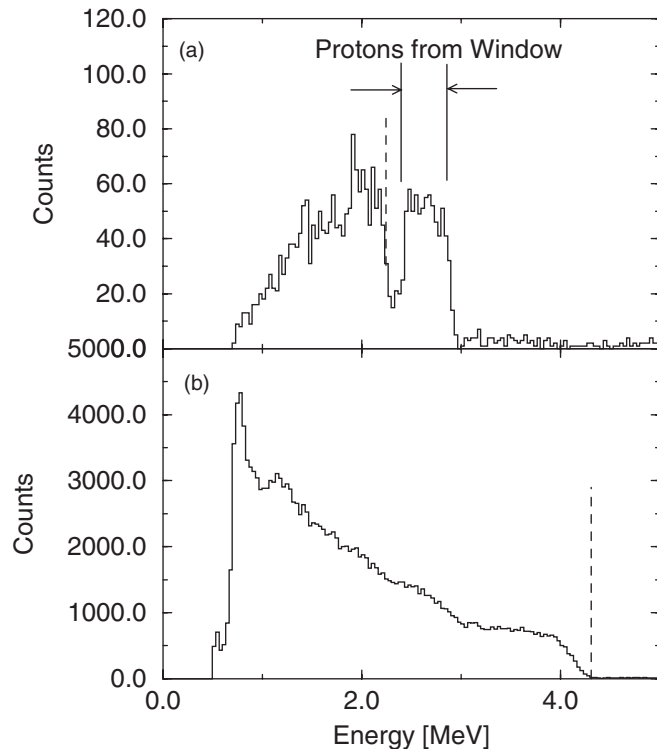
FIG. 2. (a) Proton and (b) α-particle laboratory energy spectra from the $E(^7\text{Be}) = 7.1$-MeV data. The vertical dashed lines indicate the maximum energy protons and α particles expected from the resonant scattering reactions. In part (a) the region of the spectrum corresponding to protons knocked out of the Mylar window foil is indicated.

FIG. 3. (Color online) Measured cross sections for the ^{4}He(^{7}Be, p)^{10}B (top) and ^{4}He(^{7}Be, α)^{7}Be (bottom) reactions. The red lines show the R-matrix fit to the data with $R_0 = 1.4$ fm. Blue data points indicate the high-energy data measured at ORNL and the black data points are the data from LLN. The error bars indicate statistical errors only. The green line shows the R-matrix fit with $R_0 = 1.3$ fm.

the ^{4}He(^{7}Be,^{4}He)^{7}Be data to the Rutherford scattering cross section at center-of-mass energies less than 1 MeV (see the black data points in Fig. 3).

B. $E_{\text{beam}} = 23$ MeV

A similar procedure was followed for the measurements of the ^{4}He(^{7}Be,^{4}He)^{7}Be and ^{4}He(^{7}Be, p)^{10}B reactions at the higher beam energy. On this occasion the protons were identified from the ΔE-E locus in the spectrum associated with the particle identification telescope. Unlike the protons, the α particles were stopped in the first silicon detector and hence there was no explicit particle identification and so the particles were identified from their characteristic energy. The proton and α-particle energy spectra were again normalized to account for the variation in the detector acceptance as a function of the position of the interaction in the chamber and the corresponding $E_{\text{c.m.}}(^{11}\text{C})$ were calculated. The cross sections for the two reactions were then determined by normalizing the higher energy data for the ^{4}He(^{7}Be,^{4}He)^{7}Be reaction to the $E_{\text{beam}} = 7.1$-MeV data in the region of overlap between $E_{\text{c.m.}} = 1.5$ to 2 MeV. In this region the agreement in terms of the shape of the spectra for the two measurements was very good. The resulting ^{11}C excitation function is shown in Fig. 3 as the blue data points.
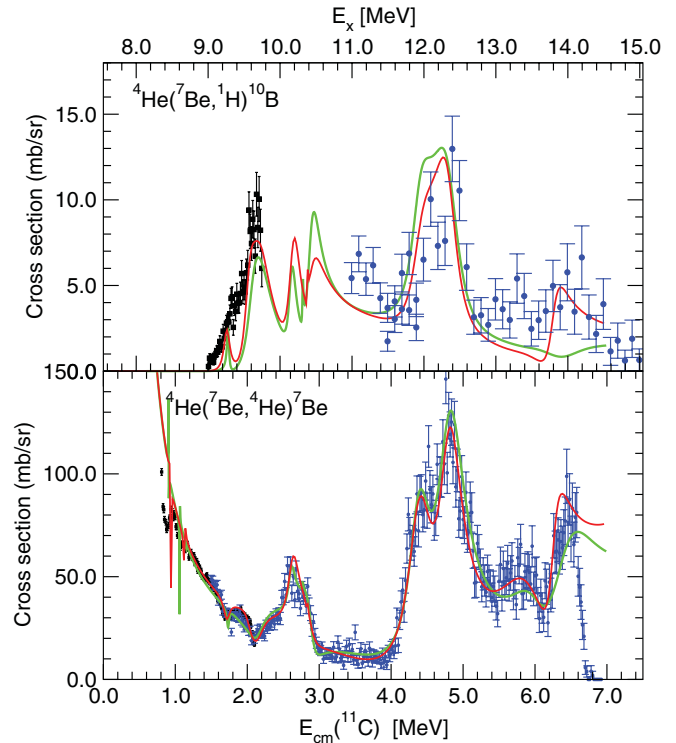
It is important to note that the calculation of the reaction cross sections relies strongly on the assumptions within the Monte Carlo calculations, particularly the assumed angular distributions. For each distance from the detector the range of center-of-mass angles intercepted varies. Hence, the assumption regarding the angular distributions will affect the normalization of the data. For the 23-MeV data it is estimated that this uncertainty introduces a systematic uncertainty of a factor of 2.5 (maximum value) in the cross section at the highest energy end of the spectra in Fig. 3 at $E_{\text{c.m.}} = 6.5$ MeV, decreasing to 1.5 at $E_{\text{c.m.}} = 4.0$ MeV.

It is possible that there is some contribution to the α-particle spectrum from the inelastic reaction ^{4}He(^{7}Be, α)^{7}Be*. However, the measurement of the analog reaction, ^{4}He(^{7}Li, α)^{7}Li* [8], indicates that this contribution has a cross section two orders of magnitude smaller. It is not clear whether this is an accurate conclusion given that an alternate measurement of the inelastic scattering indicated a larger cross section [13]. The inelastic resonant scattering spectrum shown in Fig. 4 of Ref. [8] does not indicate strong resonances. If there were strong inelastic contributions to the present spectrum they would be manifest as the resonances observed in the elastic spectrum being shifted by 0.43 MeV, the energy of the first excited state of ^{7}Be. It is not possible to rule out such contributions, but they are expected to be at a level which does
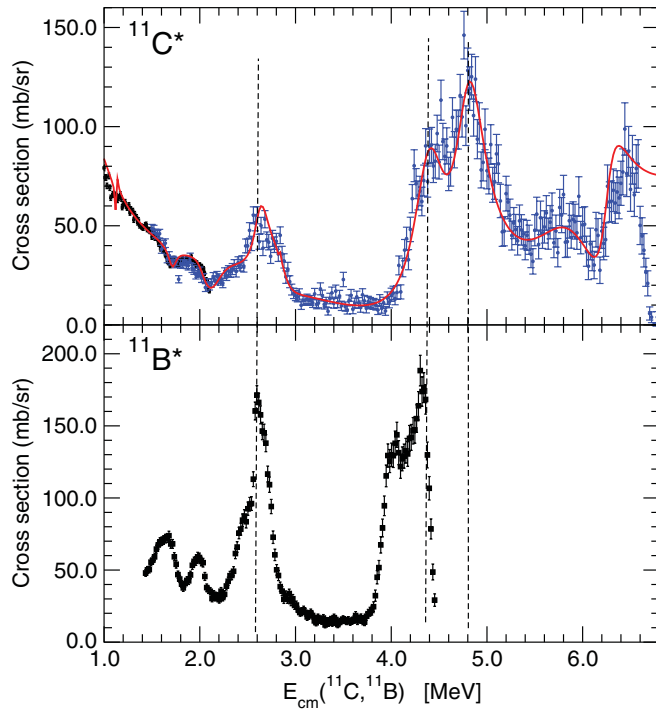
FIG. 4. (Color online) Comparison between resonant scattering of ^{7}Li $+ \alpha$ (top) from Ref. [8] and ^{7}Be $+ \alpha$ (bottom). The red line corresponds to the R-matrix fit to the data, described in the text. The vertical dashed lines are associated with the dominant features of the ^{7}Be $+ \alpha$ spectrum and are to guide the eye.

not dominate the analysis. However, further measurements are required to resolve the discrepancy between the inelastic cross sections reported in Refs. [8,13]. Similarly, contributions to the proton spectrum from the decay to first excited states in ^{10}B (0.718 MeV) cannot be excluded, though there is no obvious evidence in the spectra shown in Fig. 3 for such a reaction.

IV. *R*-MATRIX ANALYSIS

To characterize the resonances observed in Fig. 3, a series of R-matrix calculations have been performed [14,15]. These calculations simulate resonances in a nuclear potential with a radius given by $r = 1.4(7^{1/3} + 4^{1/3})$ fm (the α-particle channel radius). In the present approach, the decays to both the ^{7}Be$_{gs}$ + α and ^{10}B$_{gs}$ + p channels are included. Hence, it is possible to infer information regarding the partial decay widths Γ_α and Γ_p. The magnitude of peaks in the resulting excitation energy spectrum is proportional to $(2J + 1)\Gamma_\alpha^2$ (J being the resonance spin) and the width is given by $\Gamma = \Gamma_\alpha + \Gamma_p$. In this manner it is possible to gain an insight into the spin and partial widths of the experimentally observed resonances. In turn, the partial widths are related to the reduced widths, γ_α^2, via $\Gamma_\alpha = 2P_L\gamma_\alpha^2$ (for α decay), where P_L is the R-matrix penetrability (i.e., the barrier penetrability multiplied by kr, with k being the wave number describing the center-of-mass motion and r the channel radius described above) for a given orbital angular momentum L. The widths of the states are thus also sensitive

to the spin of the resonance via the orbital angular momentum required for the formation and the effect of the centrifugal barrier.

The results of the R-matrix calculations are shown in Table I and Fig. 3. These calculations have been guided by the tabulated energy levels of ^{11}C [16] and analysis of resonant scattering measurements of ^{7}Li $+ \alpha$ populating resonances in ^{11}B [8], which should be the analogs of those populated in the current work. The tabulated values correspond to a value of $R_0 = 1.4$ fm. In order to gain an appreciation of the uncertainties in the analysis, it has been repeated with $R_0 = 1.3$ fm. The uncertainties presented in Table I reflect the variation in the corresponding widths and partial widths.

Figure 4 also shows the comparison between the ^{7}Be $+ \alpha$ excitation function and that corresponding to ^{7}Li $+ \alpha$ from Ref. [8]. It is clear that using a combination of the adopted energy levels and those found in the ^{7}Li $+ \alpha$ measurements it is possible to produce a reasonable description of the ^{4}He(^{7}Be,^{4}He)^{7}Be and ^{4}He(^{7}Be, p)^{10}B reaction cross sections. The $E_{\text{c.m.}}$ resolutions for the proton and α-particle spectra are expected to be dominated by the resolution of the detectors (100 keV; FWHM) and hence are estimated to be 10 and 40 keV, respectively. Given this resolution it is clear that the features in the α-particle spectrum at $E_{\text{c.m.}} < 1.2$ MeV will not be reproduced, though it is possible to observe variation in the Rutherford scattering cross section, which indicate a sensitivity to these low-energy resonances. However, it is clear that in this region the spectrum is dominated by the Rutherford scattering cross section.

A. $E_{\text{c.m.}} = 1.2$ and 2.3 MeV

Between $E_{\text{c.m.}} = 1.2$ and 2.3 MeV there are two dips in the spectra associated with the ^{4}He(^{7}Be,^{4}He) reaction which are reasonably well reproduced with the known $5/2^+$ state at $E_x = 9.20$ MeV ($E_{\text{c.m.}} = 1.66$ MeV) and $(3/2^-)$ and $(5/2^-)$ states at $E_x = 9.65$ and 9.78 MeV ($E_{\text{c.m.}} = 2.11$ and 2.24 MeV), respectively. Due to the proximity to the Coulomb barrier and with an additional $L = 1$ centrifugal barrier for the α-particle decay coupled with the proximity to the proton decay threshold (8.689 MeV) it is very difficult to achieve a width of 500(100) keV as tabulated for this state. The proton spectrum (Fig. 3) clearly shows the need for a proton decay branch of a broad state at this energy. This may indicate the influence of another level not included in the present analysis. For example, a $(1/2^+)$ state is tabulated at $E_x = 9.82$ MeV for ^{11}B [16].

Close to $E_{\text{c.m.}} = 2.1$ MeV the features of the spectra can be reproduced by broad $3/2^-$ and $5/2^-$ states with widths close to those tabulated [16] for the $E_x = 9.65$ and 9.78 MeV states.

B. $E_{\text{c.m.}} = 2.3$ and 3.5 MeV

In this energy interval (corresponding to excitation energies between 9.8 and 11.0 MeV), three states were required to reproduce the α-particle spectrum. Due to restrictions in the range of proton energies detectable, it was not possible to

TABLE I. Comparison between the adopted values for states in ^{11}C [16], those from the current work (see the text for details), and analog states in ^{11}B. The numbers in italics indicate that at 12.63 MeV a series of states with the proposed spins and parities was found in Ref. [8]. The uncertainties in the calculation of the energy-loss corrections and the R-matrix analysis lead to uncertainties in the excitation and center-of-mass energies which are <100 keV. The uncertainties in the widths, given in brackets, were determined by a comparison with an R-matrix analysis with $R_0 = 1.3$ fm.

Adopted values [16]			Current Work										Proposed ^{7}Li $+ \alpha$ analogs [8]		
E_x (MeV)	J^π	Γ (keV)	$E_{c.m.}$ (MeV)	E_x (MeV)	J^π	L_α ($\hbar$)	L_p ($\hbar$)	Γ_α (keV)	Γ_p (keV)	Γ (keV)	$\frac{\Gamma_\alpha}{\Gamma_W}$ %	E_x (MeV)	J^π	Γ_α (keV)
8.699	$5/2^+$	15(1)	1.10	8.65	$5/2^+$	1	0	1(1)		1(1)	1			
9.20	$5/2^+$	500(100)	1.63	9.18	$5/2^+$	1	0	12(7)	96(42)	108(43)	2			
9.65	$(3/2^-)$	210(50)	2.09	9.64	$3/2^-$	0	1	156(20)	222(52)	378(56)	10	10.24	$3/2^-$	4
9.78	$(5/2^-)$	240(60)	2.08	9.63	$5/2^-$	2	1	54(41)	217(44)	271(60)	13	10.34	$5/2^-$	19(4)
10.083	$7/2^+$	230	2.59	10.14	$7/2^+$	3	0	28(5)	117(27)	145(13)	12	10.60	$7/2^+$	10(3)
												11.06	$5/2^+$ $(3/2^+,7/2^+,9/2^+)$	32(20)
10.679	$9/2^+$	200(30)	3.03	10.58	$9/2^+$	3	2	13(10)	42(19)	55(22)	3	11.29	$9/2^+$	35(4)
			2.96	10.50	$7/2^-$	2	1	92(41)	214(51)	306(65)	8	(11.59)	$(7/2^-)$	270
			4.44	11.99	$7/2^+$	3	0	365(103)	102(43)	467(112)	25	*12.63*	*$(3/2^+, 5/2^+, 7/2^+, 9/2^+)$*	*33–400*
			4.86	12.40	$9/2^+$	3	2	452(74)	90(35)	542(82)	25	*12.63*	*$(3/2^+, 5/2^+, 7/2^+, 9/2^+)$*	*33–400*
												13.03	$9/2^-$	140
			5.88	13.42	$5/2^+$	1	0	734(65)	8(8)	743(66)	15			
			6.26	13.80	$5/2^-$	2	1	330(540)	332(234)	662(585)	8			

measure the proton energy spectrum and hence there are no data to constrain the proton decay widths. There are two key states in this region: the 10.083-MeV $7/2^+$ and the 10.679-MeV $9/2^+$. The R-matrix analysis including such resonances produces a fit which is broadly consistent with the adopted values [16]. An additional resonance at $E_{c.m.} = 2.96$ MeV ($E_x = 10.50$ MeV) with spin and parity $7/2^-$, as employed in the analysis of the ^{7}Li $+ \alpha$ reaction [8], is required to reproduce the shape of the spectrum in this region.

C. $E_{c.m.} = 3.5$ and 5.2 MeV

In this energy interval, corresponding to excitation energies between 11.0 and 12.7 MeV, the R-matrix analysis has been guided by that performed for the ^{7}Li $+ \alpha$ measurements (see Table I). This latter analysis indicated that positive-parity states associated with $L_\alpha = 3$ ($3/2^+$, $5/2^+$, $7/2^+$, and $9/2^+$) dominated this region. A higher energy negative-parity state ($9/2^-$) was required to produce the sharp fall-off at the high-energy end of the spectrum (see Fig. 4). It is possible that this feature is an effect of the high-energy cutoff imposed by the maximum energy of the measurement rather than a reduction in the cross section—certainly the ^{7}Be $+ \alpha$ reaction shows no such strong feature. In the present analysis it is possible to reproduce the proton and α-particle spectra with $7/2^+$ and $9/2^+$ states at $E_x = 11.99$ and 12.40 MeV, respectively ($E_{c.m.} = 4.44$ and 4.86 MeV). This is the preferred assignment, though it is possible that the ordering of the $7/2^+$ and $9/2^+$ states could be inverted with only a slightly worse fit to the data. Higher quality proton data may help to resolve this ambiguity. It should be noted that there are two possible spin couplings for the proton decay to the ^{10}B(3^+) $+ p(1/2^+)$: $S = 5/2$ or $7/2$. The R-matrix calculation shown in Figs. 3 and 4 is the average of these two possibilities.

D. $E_{c.m.} > 5.2$ MeV

Above $E_{c.m.} = 5.2$ MeV ($E_x = 12.7$ MeV) there are few constraints from other measurements on the nature of the spectrum in this region. In the present analysis we find that the spectrum can be produced by broad $5/2^+$ and $5/2^-$ states, though this is unlikely to be a unique possibility.

V. DISCUSSION

In Ref. [6] a number of ^{11}C states were observed via the ^{16}O(^{9}Be,^{7}Be $+ \alpha$)^{14}C, transfer then breakup reaction. In particular, strong states were found at 8.65, 9.85, 10.7, and 12.1 MeV with an indication of weaker states at 12.6 and 13.4 MeV. It was proposed that these states were associated with rotational bands with $K^\pi = 3/2^+$ and $5/2^+$ character and that the 12.1-MeV state was associated with the $J^\pi = 7/2^+$ member of the $K^\pi = 3/2^+$ band and the 12.6-MeV state with the $9/2^+$ member of the $K^\pi = 5/2^+$ band. Presumably, the 12.1- and 12.6-MeV states corresponds to the 11.99- and 12.40-MeV states in the current data. If the assignments in Ref. [6] are correct then this would correspond to the possible inversion of $7/2^+$ and $9/2^+$ states mentioned above. Clearly, direct measurement of the spins of the states would help clarify the energy ordering of the probable $7/2^+$ and $9/2^+$ states.

In order to characterize the nature of the resonances as determined from the R-matrix analysis the α-particle width has been compared with the Wigner limit [$\Gamma_W = 2 P_L \gamma_W^2$; $\gamma_W^2 = 3\hbar^2/2\mu r^2$, with μ being the reduced mass, $r = 1.4(4^{1/3} + 7^{1/3})$, and P_L the R-matrix penetrability]. The comparison to this limit provides a measure of the relative degree of α-particle clusterization associated with the resonance. This would indicate that the states with the largest degree of clustering are the proposed $E_x(^{11}$C$) = 11.99$-MeV $7/2^+$ and

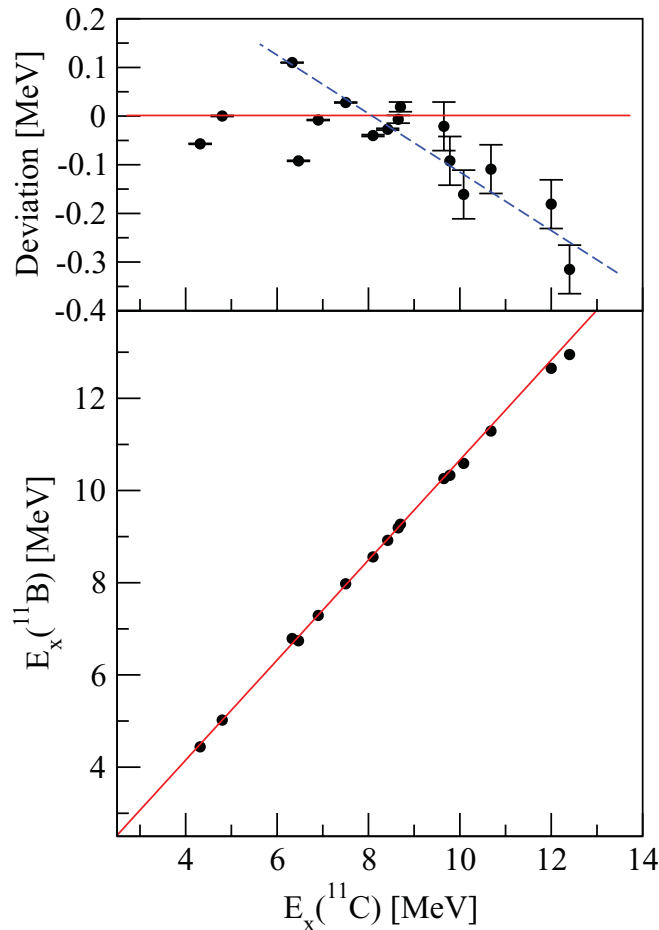FIG. 5. (Color online) Comparison between excitation energies of ^{11}C and ^{11}B states (lower panel). The red line is a linear fit to the states associated with ^{11}C excitations between 4 and 9 MeV. The top panel shows the deviation from the linear fit. The blue dashed line indicates the locus of the states which are proposed to be linked with excitations to the *sd* shell (see the text for details).

12.40-MeV $9/2^+$ states. The comparison with a similar analysis performed for the ^{11}B resonances populated through the ^{7}Li + α reaction [8] is significant. The ^{7}Li + α data indicate that most of the resonances have significant clusterization as measured against the Wigner limit and is again large for the proposed $7/2^+$ and $9/2^+$ states close to $E_x(^{11}$B$) = 12.63$ MeV. This would point to a cluster origin for the structures close to this energy in both nuclei. However, the spins of these states cannot be firmly assigned through the present analysis; only a consistency between proposed widths, spin, and partial widths and experimental cross sections could be observed. Angular distribution measurements are required to provide firm assignments.

A comparison can be made which does not rely on a detailed knowledge of the spins, as illustrated in Fig. 4. The structure of the two spectra populated in the two reactions is strikingly similar. As indicated by the vertical dashed lines, measured with respect to the α-decay thresholds (with α-particle decay thresholds in ^{11}C and ^{11}B being 7.544 and 8.655 MeV, respectively), there is close alignment in energy of the peaks

around $E_{c.m.} = 2.6$ MeV, whereas the higher energy structure is shifted by $\sim$400 keV to higher energies. Figure 5 shows the comparison of known analog states in ^{11}C and ^{11}B between 4 and 10 MeV together with the $7/2^+$ states at 10.083 MeV in ^{11}C and 10.59 MeV in ^{11}B and the $9/2^+$ states at 10.68 and 11.29 MeV in ^{11}C and ^{11}B, respectively. In addition, the energies of the two states at $E_x(^{11}$C$) = 4.4$ and 4.8 MeV are included. The data are well represented by a straight line aside from these latter higher energy states. The red line shows a linear fit up to $E_x(^{11}$C$) = 8.65$ MeV and the top part of the figure shows the deviation from the fit. It would appear that for the higher energy states the excitation energy is systematically higher for ^{11}C than for ^{11}B, relative to the lower energy states. This deviation may signal a change in structure of these highest energy states. It is possible that such a deviation is associated with the clustered nature of the states. Such behavior has been explored by Wildermuth and co-workers for a range of light nuclei [17,18]. In the present instance, following the prescription in Ref. [19], the Coulomb energy difference between the two spherical ^{11}C and ^{11}B nuclei is 2.7 MeV (with the experimental difference in the ground-state energy being $\sim$2.0 MeV). For a clustered state formed from $2\alpha + {}^3$He$(^3$H$)$ with the clusters in a triangular arrangement separated by their radii, the energy difference is calculated to be 2.3 MeV. In other words, there is a gain in binding energy for ^{11}C compared to ^{11}B in going from the nonclustered to the clustered state. This is indeed seen: at $E_x \approx 8$–9 MeV the slope of the line connecting the data points in Fig. 5 (lower part) abruptly becomes smaller (but still greater than one), indicating a "phase change" in which states shift from shell-model-like ("liquid phase" in Ref. [20]) to cluster ones ("solid phase" in Ref. [20]). From the lowest cluster states, most of the higher lying levels are just members of the same rotational band (or its parity doublet), having more or less the same geometry—this is the reason why their radii, and therefore the Coulomb energy difference between the ^{11}C and ^{11}B mirrors, show much slower growth with excitation energy compared to the shell-model states.

However, it should be noted that such energy shifts are influenced by both the structure and nuclear spin. Figure 6 shows the excitation difference between the ^{11}C and ^{11}B states $[E_x(^{11}$C$) - E_x(^{11}$B$)]$ as a function of the spin of the state. There is some spin dependence, but beyond that it would appear the states separate out into three groups. The ground state, the $E_x(^{11}$B$) = 2.12$ MeV ($1/2^-$), 4.44 MeV ($5/2^-$), 5.02 MeV ($3/2^-$), and 6.74 MeV ($7/2^-$) states, and then a series of states with positive and negative parity. The ground state is associated with 10 nucleons coupled to 0^+ and an unpaired $p_{3/2}$ proton or neutron (for ^{11}C and ^{11}B, respectively). The group of four states (blue diamonds) is associated with the recoupling of the nucleons in the ^{10}B core to 2^+, which is then coupled to the $p_{3/2}$ proton- or neutron-forming states $1/2^-$, $3/2^-$, $5/2^-$, and $7/2^-$. These states have a shell-model-like character. Positive-parity states can only be generated by promoting nucleons to the *sd* shell. In ^{12}C (which has one nucleon more) this is associated with the onset of clustering. The fact that there are groups of positive- and negative-parity states, all with similar excitation energy differences, would appear to indicate that they have a similar
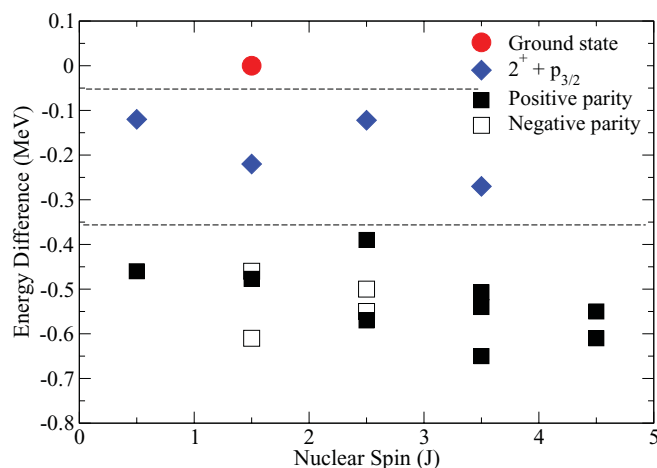
FIG. 6. (Color online) Excitation energy difference between analog states in ^{11}B and ^{11}C as a function of the spin of the state J (see text for details). The horizontal dashed lines indicate regions associated with different nuclear configurations.

structure, possibly of cluster character. In this instance, the positive-parity states would be associated with the excitation of ^{3}He or ^{3}H (for ^{11}C and ^{11}B, respectively) to the sd shell and the negative parity linked to a ^{4}He excitation to the sd shell. The appropriate line connecting states of a similar character is the blue dashed line in Fig. 5. Figure 6 shows that the excitation energy of the proposed cluster states (or at least states with an sd character) in ^{11}C is on average lower than the shell-model candidates, measured with respect to ^{11}B. This would be in agreement with the shell-model states having a more compact structure. The simple calculations for the change in the Coulomb energy between the compact and clustered state indicates an energy difference of 400 keV. The energy difference seen in Fig. 6 is closer to 500 keV. It is clear

that more sophisticated calculations would be appropriate and may lead to a clearer insight into the degree of clusterization.

VI. SUMMARY

The ^{4}He(^{7}Be, α)^{7}Be and ^{4}He(^{7}Be, p)^{10}B reactions have been measured using the thick target approach and beam energies of 7.1 and 23.0 MeV. These data provide information over the ^{11}C excitation energy range of 8.5 to 13.5 MeV. This is the first measurement of ^{7}Be + ^{4}He resonance scattering where the α-decay and proton-decay channels have been measured simultaneously. The current data overlap the well-characterized excitation energy region of 8.5 to 11.7 MeV and in general good agreement is found but there is an indication for the need of a additional $1/2^+$ resonance close to 9.2 MeV. The current measurements provide an indication of the widths Γ_α and Γ_p. Above 11.7 MeV an R-matrix analysis indicates that, in addition to known states in this region, $7/2^+$ and $9/2^+$ states exist at 11.99 and 12.40 MeV, respectively. This is consistent with measurements of the ^{7}Li + α resonant scattering populating resonances in ^{11}B over a similar energy range. It is probable that these resonances are associated with deformed cluster rotational bands, given their significant α partial widths compared with the Wigner limit and the difference in excitation energy between analog states in ^{11}C and ^{11}B.

[1] R. B. Wiringa, S. C. Pieper, J. Carlson, and V. R. Pandharipande, Phys. Rev. C **62**, 014001 (2000).
[2] M. Freer *et al.*, Phys. Rev. C **80**, 041303(R) (2009).
[3] T. Yamada and Y. Funaki, Phys. Rev. C **82**, 064315 (2010).
[4] A. Kabir and B. Buck, Nucl. Phys. A **533**, 215 (1991).
[5] Y. Kanada-Enyo, Phys. Rev. C **75**, 024302 (2007).
[6] N. Soic *et al.*, Nucl. Phys. A **742**, 271 (2004).
[7] N. Curtis, N. I. Ashwood, W. N. Catford, N. M. Clarke, M. Freer, D. Mahboub, C. J. Metelko, S. D. Pain, N. Soic, and D. C. Weisser, Phys. Rev. C **72**, 044320 (2005).
[8] H. Yamaguchi *et al.*, Phys. Rev. C **83**, 034306 (2011).
[9] K. P. Artemov *et al.*, Sov. J. Nucl. Phys. **52**, 406 (1990).
[10] T. Davinson *et al.*, Nucl. Instrum. Methods A **454**, 350 (2000).

[11] Micron Semiconductor Ltd., 1 Royal Buildings, Marlborough Road, Churchill Industrial Estate, Lancing, Sussex BN15 8UN, UK.
[12] Energy loss code DEDX (unpublished).
[13] H. Bohlen, N. Marquardt, W. von Oertzen, and P. Gorodetzky, Nucl. Phys. A **179**, 504 (1972).
[14] A. M. Lane and R. G. Thomas, Rev. Mod. Phys. **30**, 257 (1958).
[15] R-matrix code courtesy of G. Rogachev.
[16] F. Ajzenberg-Selove, Nucl. Phys. A **506**, 1 (1990).
[17] K. Wildermuth and Y. C. Tang, Phys. Rev. Lett. **6**, 17 (1961).
[18] K. Wildermuth and E. J. Kanellopoulos, Rep. Prog. Phys. **42**, 1719 (1979).
[19] K. Wildermuth and Y. C. Tang, *A Unified Theory of the Nucleus* (Vieweg, Braunschweig, Germany, 1977), p. 322.
[20] N. Itagaki, H. Masui, and J. Cseh, J. Phys. Conf. Ser. **111**, 012006 (2008).